Tr. J. of Physics
22 (1998) , 929 – 937.

Structural and Optical Characterisation of Vacuum Deposited CdTe Thin Films

Murat BAYHAN
Muğla University, Faculty of Arts and Science
Physics Department, 48000, Muğla - TURKEY

Received 16.10.1997

Abstract

The structural and optical properties of vacuum deposited CdTe thin films on glass substrates were investigated. The effect of the heat treatment in air over the former properties of the layers was also examined. Grain sizes of air heated layers estimated by net broading in the XRD spectra were found to be larger than as-grown layers, confirming that grain growth had occurred during the heat treatment. RHEED patterns of the layers grown at substrate temperatures between 150°C and 170°C had a distinct {111} preferred orientation. As-grown CdTe layers were slightly p-type, but highly resistive. Air heat treated layers were p-type and slightly less resistive than as-grown layers, possibly due to oxygen related Cd vacancy formation. Optical bandgap values, determined by envelope function model, were found to be 1.53 eV and 1.51 eV for as-grown and heat treated layers, respectively.

1. Introduction

CdTe has long been identified as a candidate for the absorber layer in low cost thin film photovoltaic solar cells because of its direct bandgap, high absorption coefficient, its ability to be doped both n- and p-type and the possibility of a variety of preparation techniques such as vacuum deposition [1,2], electrodeposition [3,4], molecular beam epitaxy [5,6], metal-organic chemical vapour deposition [7,8], close-space sublimation [9,10] and screen printing [11,12]. In the 1960's, the first CdTe based solar cells with efficiencies of 4-6% were reported by Vodakov et.al. [13] and Nikolaev [14]. Due to difficulties of forming a thin film shallow junctions with highly conducting surface layers, heterojunction cells where CdS and/or (Cd, Zn)S as a window layer were developed and have proved to be efficient and stable. Development led to best efficiencies in the range of 12-16% [15,16,17]. An overview of the CdTe thin films have been written by Basol, Bonnet and Chu [18,19,20].

Cell performance is closely related to detailed understanding of morphology, crystallinity and optical behaviour of the individual layers forming the cell. Therefore, in this work, structural and optical assessments of CdTe layers grown on cleaned glass substrates by vacuum deposition were investigated.

2. Experimental Procedure

The CdTe thin films were deposited onto cleaned glass substrates by vacuum evaporation. The layers were generally grown with source and substrate temperatures between $650 - 800°C$ and $150 - 250°C$, respectively. Selected layers were also heat treated in air, usually for 30 min. at 400°C. This is an essential process frequently used in CdTe based solar cell fabrication for obtaining a CdTe layer with a higher p-type conductivity and with improved crystallinity. The RHEED patterns from the surfaces of the layer were obtained using a JEM 120 TEM fitted with a RHEED stage. The surface and cross sectional morphologies and compositional analysis of the layers were performed using a Cambridge Stereoscan S600 SEM fitted with a link system of EDAX analyser. A Philips PW1130, generator/diffractometer assembly employing a Cu anode was used for XRD analysis. SIMS analysis was also carried out using facilities provided by BP Solar in order to identify elemental proportion of the composition through the depth of the layer.

The normal incidence optical transmission spectra were obtained by a double beam Perkin-Elmer Lambda 19 UV/VIS/NIR spectrophotometer, and were taken with reference to air at room temperature.

3. Results and Discussion

3.1. X-Ray Diffraction Assessments

Figure 1a shows the x-ray diffraction trace using Ni-filtered $Cu_{k\alpha}$ radiation with a wavelength of $\lambda = 1.518\mathring{A}$ from an as-grown CdTe thin film. Although the diffraction peaks at $2\theta_B$ angles of $23.8°, 46.4°, 76.2°$ are associated with corresponding planes of cubic CdTe, the peaks at $2\theta_B$ angles of $23.1°, 25.9°, 29.6°$ and $32.6°$ could not be so identified. Their origin is not known, but this could be oxygen reacting with free deposits of Te accumulated on the surface due to the higher vapour pressure of Cd in vacuum evaporation [21].

Annealing the CdTe thin layers at 400°C for about 30 min. in air showed a dramatic change in the x-ray diffraction spectra, as shown in Figure 1b. The intensity of the diffraction peak associated with the {111} planes of cubic CdTe increased due, possibly, to grain growth resulting in a greater degree of preferred ordering. In addition, the rate of increase in the intensity of the peak associated with the {511} planes as in the as-grown case, was also found to be significant.

For a typical thin layer of cubic CdTe, the lattice parameter a_0 was estimated to be

6.48 Å by using the equation [22]:

$$\sin^2\theta_B = \frac{\lambda^2}{4a_0^2}(h^2+k^2+l^2), \tag{1}$$

where (hkl) are the Miller indices and λ is the particular incident wavelength of the radiation.

X-ray diffraction was also used to obtain the estimates of grain size (i.e. crystallite size) in the CdTe thin films. The method relies on the fact that small grains produce line broadening in x-ray diffraction spectra. In order to distinguish the line broadening observed in principal diffraction peaks associated with small grain size from that due to the instrument, a reference XRD spectrum was taken from a bulk single crystal of GaAs. The net broadening, β_{hkl}, is

$$\beta_{hkl} = \sqrt{B_{hkl}^2 - b_{hkl}^2}, \tag{2}$$

where B_{hkl} is the measured line width (FWHM) and b_{hkl} is the instrumental broadening. The grain size ϵ_{hkl} can then be obtained as [23]

$$\epsilon_{hkl} = \frac{K\lambda}{\beta_{hkl}\cos\theta_B}, \tag{3}$$

where K is a shape factor and is utilized to take account of the crystallite shape factor and orientation, with an average value of 0.9 is generally used for polycrystalline films; and θ_B is the Bragg angle.

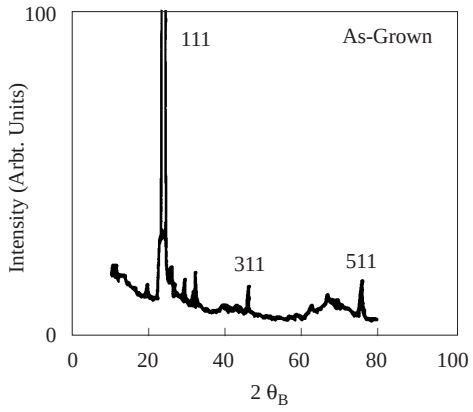

Figure 1a. X-ray diffraction spectrum of an as-grown CdTe thin film.

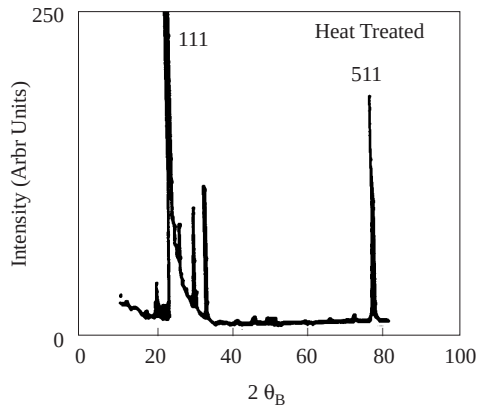

Figure 1b. X-ray diffraction spectrum of a heat treated CdTe thin film.

Grain sizes for the as-grown CdTe thin layers were estimated to be 78-85 nm, and for thin layers annealed in air at 400°C for about 30 min. The average grain size was

estimated to be ∼100 nm. This suggests that some limited grain growth had occurred during the heat treatment in air. This is a comparatively low temperature for grain growth/re-crystallization to occur even in a film, suggesting that grain growth may be more accelerated in the presence of oxygen.

3.2. RHEED Assessments

Reflection high energy electron diffraction (RHEED) patterns were obtained from the surfaces of CdTe thin layers grown on glass substrates in order to determine the crystal degree of preferred orientation of crystallites at the surface. The RHEED patterns of the CdTe thin films were indexed in the usual way by combining the equation for inter-planar spacing d_{hkl} and the Camera equation [24]. Hence for one set of $\{hkl\}$ planes, it can be written as

$$R_{hkl}\frac{a_0}{\sqrt{N_{hkl}}} = \lambda L, \tag{4}$$

where $N_{hkl} = h^2+k^2+l^2$ and R_{hkl} is the radial distance from the central (i.e. undiffracted) spot. Thus for two sets of planes (hkl) and (h′k′l′), one obtains;

$$\frac{R_{hkl}}{R_{h'k'l'}} = \frac{\sqrt{N_{hkl}}}{\sqrt{N_{h'k'l'}}} = \frac{d_{hkl}}{d_{h'k'l'}}. \tag{5}$$

Comparison of the ratios of experimentally observed arc radii (i.e. with respect to the first and brightest arc associated with {111} planes) yielded $\sqrt{N_{hkl}}$ ratios without the necessity for a calibration standard. The surface of layers grown at substrate temperatures ≥ 180°C had a random polycrystalline texture with a weaker preferred orientation along the {111} planes although layers grown at substrate temperatures ≤ 170°C had a distinct {111}-preferred orientation which was stronger at the lower substrate temperatures.

Figure 2 shows the indexed pattern for a typical as-grown CdTe thin film grown at a substrate temperature of 150°C on a glass substrate. The indexing was confirmed by comparing the measured angle subtended by a given arc with respect to the normal through the principal {111} arc with the calculated value. These are related to the respective Miller indices by the equation [22]:

$$\cos\phi = \frac{h_1h_2 + k_1k_2 + l_1l_2}{\sqrt{(h_1^2 + k_1^2 + l_1^2)(h_2^2 + k_2^2 + l_2^2)}}. \tag{6}$$

All of the measured and calculated angles were in good agreement with the indices in Figure 2, and it was concluded that the film is polycrystalline and the arc pattern contained diffracted intensity analogous to the [112] and [110] beam directions and {111} planes were parallel to the substrate (i.e. there is a {111} preferred orientation).

The RHEED patterns of the heat treated CdTe layers were also investigated. The patterns of arcs were almost identical to those of as-grown {111} oriented CdTe layers, except for an additional arc which was located just above the {111} arc. Calculation of the d-spacing for this arc yielded a value of 3.24 Å which corresponds closely to the values of d-spacing for either Te or TeO_2.

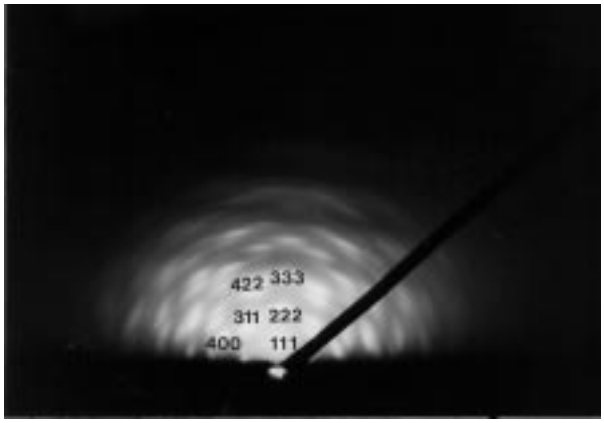

Figure 2. RHEED pattern from an as-grown CdTe thin film grown on glass at a substrate temperature of 150°C.

3.3. SEM Assessments

Routine assessment of the surface morphology of the thin films was performed using the secondary electron (SE) mode of a SEM. As-grown CdTe thin layers showed a smooth surface (see Figure 3a). They displayed columnar growth, with the growth axis tilted by about $\sim 15^\circ$ to the substrate normal, as shown by the cross section in Figure 3b.

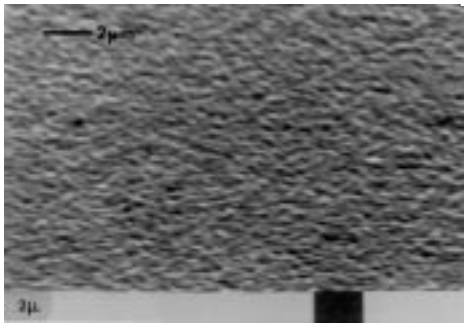

Figure 3a. Secondary emission micrograph of an as-grown CdTe thin layer surface grown on a glass substrate.

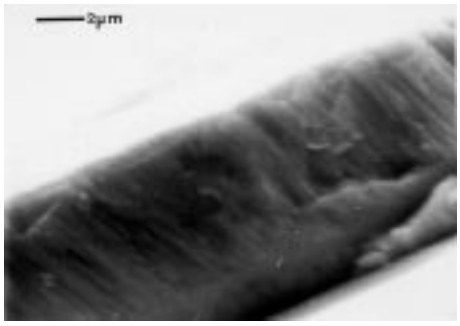

Figure 3b. Secondary emission micrograph of a cross section through an as-grown CdTe thin film grown on a glass substrate.

EDAX scans (see Figure 4) confirmed that as-deposited undoped CdTe layers comprised only Cd and Te. No other elements were observed within the limits of sensitivity (i.e. elements with atomic number less than 11 or with concentrations less than 1% would not be detected by EDAX scans).

3.4. Secondary Ion Mass Spectroscopy (SIMS)

The quality of a layer depends on the uniformity of the individual components throughout the depth of the layer. Hence, a depth profile assessment by SIMS was undertaken to investigate the concentration of Cd and Te through the depth of the layer. Figure 5 shows a depth profile for the Cd and Te of a typical heat treated CdTe layer. It displayed nearly a stoichiometric CdTe with a higher Cd concentration near to the glass interface (i.e. first a few layers contained more Cd than Te).

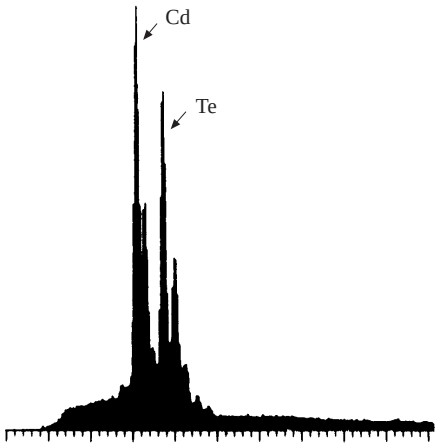

Figure 4. EDAX scan of an as-grown CdTe thin layer surface grown on a glass substrate.

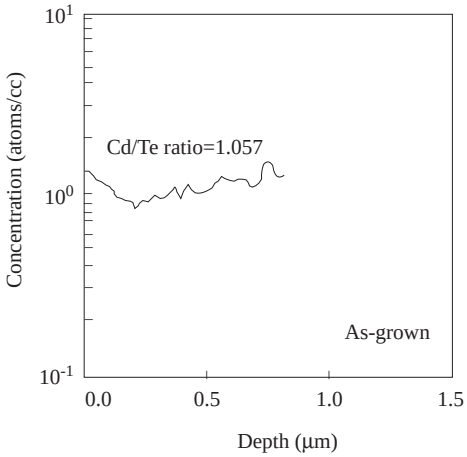

Figure 5. SIMS depth profile of an as-grown CdTe thin film grown on a glass substrate.

3.5. Spectrophotometric Assessments

Figures 6a and 6b show transmission spectra for typical as-grown and heat treated CdTe layers, respectively. Both show good transparency (T≥80%) exhibiting interference pattern in the spectral region between 0.9-2.5 μm and display a clear explicit absorption edge interrelated to the optical bandgap. This was much sharper and had shifted to longer wavelengths as in the heat treated layers.

The absorption coefficient as a function of photon energy was determined by envelope function model [25,26,27]. Employing the assumption that the transition probability becomes constant near the band edge, the absorption coefficient for the allowed direct transitions may, in general, be written as a function of photon energy as [28]:

$$\alpha \propto \left(\frac{hv - E_g}{hv}\right)^{1/2}, \tag{7}$$

in which E_g is the bandgap and hv is the photon energy.

Figure 7 shows the variation of $(\alpha hv)^2$ against photon energy obtained from the as-grown and heat treated CdTe layers. Bandgap values were obtained as 1.53 eV and 1.51

eV for the as-grown and heat treated layers, respectively. The shift observed at absorption edge towards lower photon energies for the heat treated layers could be attributed to the change in the grain size and the stoichiometry due to loss of Cd resulting formation of shallow acceptor levels [29,30]. The bandgap value of heat treated layers was also found to be in good agreement with those published in the literature for bulk CdTe [31-33].

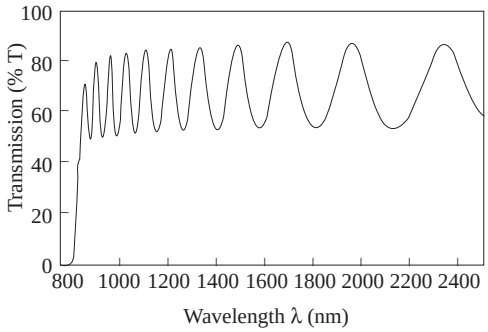

Figure 6a. Normal incidence transmission spectra for a typical as-grown CdTe thin layer grown on a glass substrate.

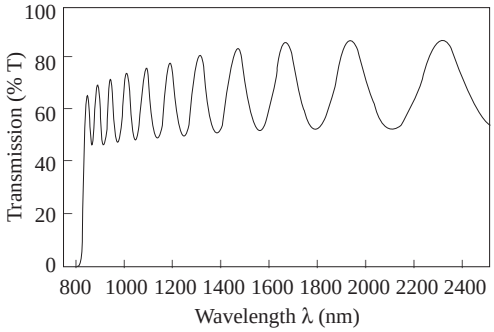

Figure 6b. Normal incidence transmission spectra for a typical as-grown CdTe thin layer grown on a glass substrate.

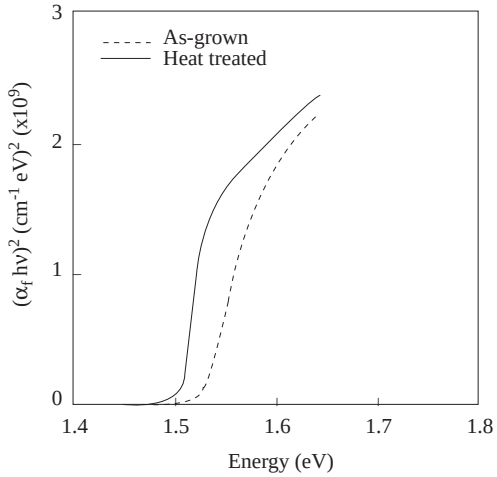

Figure 7. $(\alpha hv)^2$ vs hv characteristics of as-grown (dashed) and heat treated (continuous line) layers.

4. Conclusion

The XRD revealed that the layers were {111} preferred oriented. Heat treatment in

air resulted in a small increase in grain size. In addition, there were peaks (relatively small in intensity) associated with possibly pure Te or TeO_2.

RHEED patterns of the as-grown layers had a distinct {111} preferred orientation, as well as heat treated layers, except that an additional arc, located above {111} arc appeared. This could be associated with either Te or TeO_2. The layers displayed columnar growth with the growth axis tilted to the substrate normal and showed a smooth surface. EDAX scans also confirmed that undoped CdTe layers comprised only Cd and Te. A depth profiling by SIMS also showed that layers were nearly stoichiometric. Heat treated layers exhibited much sharper band edge. This could be attributed to the increased grain size and the change in the stoichiometry due to the loss of Cd. The optical bandgap values for as-grown and heat treated layers were found to be 1.53 eV and 1.51 eV, respectively.

Acknowledgements

The author, M. Bayhan, is grateful to Dr. A. W. Brinkman Dr. K. Durose, Dr. J. Lewis and Dr. E. Özcan for their valuable guidance and many useful suggestions.

References

[1] R.W. Birkmire, B.E. McCandles and S.S. Hegasus, Int. J. Solar Energy, **12** (1992) 145.

[2] H. Bayhan and Ç. Erçelebi, Semicond. Sci. Technol., **12** (1997) 600.

[3] P.V. Meyers and C.H. Liu, Proc. 8th Photovoltaic Solar Energy Conf. (1988) 1588.

[4] W. Song, D. Mao, Y. Zhu, J. Tang and J.U. Trefny, 25th IEEE Photovoltaic Specialist Conf., (1996) 873.

[5] S.A. Ringel, A.W. Smith, M.H. MacDougal and A. Rohatgi, J. Appl. Phys., **70** (1991) 881.

[6] A.N. Týwari, H. Zagg, S. Blunier, K. Kessler, C. Maissen and J. Masek, Int. J. Solar Energy, **12** (1992) 187.

[7] T.L. Chu, S.S. Chu, C. Ferekides, J. Britt and C.Q. Wu, J. Appl. Phys., **71** (1992) 3870.

[8] A. Rohatgi, Int. J. Solar Energy, **37** (1992) 37.

[9] Y.Y. Loginov, K. Durose, H.M. Al Alhak, S.A. Galloway, S. Oktik, A.W. Brinkman, H. Richter and D. Bonnet, J. Crystal Growth, **161** (1996) 159.

[10] A. Aguilar, A.I. Oliva, R. Castro-Rodriquez, J.L. Pena, Thin Solid Films, **293** (1997) 149.

[11] N. Suyama, T. Arita, Y. Nishiyama, N. Wueno, S. Kitamura and M. Murozona, Proc. 5th Int. Photovoltaic Sci. Eng. Conf., (1990) 757.

[12] I. Clemminck, M. Burgelman, M. Casteleyn and B. Depuydt, Int. J. Solar Energy, **12** (1992) 67.

[13] Yu, A. Vodakov, G.A. Lomakina, P. Naumov and Yu P. Maslakovets, Sov. Phys. Solid State, **2** (1960) 1.

[14] G.P. Naumov and O.V. Nikolaev, Sov. Phys. Solid State, **3** (1962) 2718.

[15] J.M. Woodcock, A.K. Turner, M.E. Özsan and J.G. Summers, 22nd IEEE Photovoltaic Specialist Conf., (1991) 842.

[16] J. Britt, C. Ferekides, Appl. Phys. Lett., **62** (1993) 2851.

[17] J. Tang, D. Mao, L. Feng, W. Song and J.U. Trefny, 25th IEEE Photovoltaic Specialist Conf., (1996) 925.

[18] B.M. Basol, Doğa Turkish J. Phys., **16** (1992) 107.

[19] D. Bonnet, Int. J. Solar Energy, **12** (1882) 1.

[20] T.L. Chu, S.S. Chu, Solid State Electronics, **38**, No:3 (1995) 533.

[21] A. Dawar, K.V. Ferdinand, C. Jagdish, P. Kumar and P.C. Mathur, J. Phys. D. in Appl. Phys. **16** (1983) 2349.

[22] B.D. Cullity, Elements of X-Ray Diffraction, (Addison Wesley, New York, 1956), pp.91, 502.

[23] H.P. Klug and L.E. Elaxander, X-Ray Diffraction Procedures, (John Wiley & Sons, New York, 1954) p.687.

[24] G. Russell, Prog. Crystal Growth and Charact., **5** (1982) 291.

[25] J.C. Manifacier, M. Demurcia, J.P. Fillard and L. Vicaria, Thin Solid Films, **41** (1977) 127.

[26] R. Swanepoel, J. Phys. E. Sci. Instrum., **16** (1985) 1214.

[27] Yeuh-Yeong Liou, Cheng-Chung Lee, Cheng-Chung Jaing, Chen-Wei Chu and Jin-Cherng Hsu, Jpn. J. Appl. Phys., **34** (1995) 1952.

[28] J.I. Pankove, Optical Process in Semiconductors, (Prentice Hall, Inc., New Jersey, 1971) p.36.

[29] R.F.C. Farrow, G.R. Jones, G.M. Williams, I.M. Young, Appl. Phys. Lett., **39** (1981) 954.

[30] D.H. Levi, H.R. Moutinho, F.S. Hasoon, B.M. Keyes, R.K. Ahrenkiel, M.Al-Jassim, L.L. Kazmerski and R.W. Birkmire, Solar Energy Materials and Solar Cells, **41** (1996) 381.

[31] P.J. Olega, J.P. Faurie, S. Sivananthan and P.M. Raccah, Appl. Phys. Lett., **47** (1985) 1172.

[32] W.S. Enloe, J.C. Parker, J. Vespoli, T.H. Meyers, R.L. Harper and J.F. Schetzina, J. Appl. Phys., **61** (1987) 2005.

[33] A.N. Pikhtin and A.D. Yaskov, Sov. Phys. Semicond. **22** (1988) 613.